Cement & Concrete Composites 34 (2012) 746–753

Contents lists available at SciVerse ScienceDirect

Cement & Concrete Composites

journal homepage: www.elsevier.com/locate/cemconcomp

Effect of powder materials on the rheology and formwork pressure of self-consolidating concrete

Jae Hong Kim [a,*], Nagy Noemi [b], Surendra P. Shah [c]

[a] School of Urban and Environmental Engineering, Ulsan National Institute of Science and Technology, Republic of Korea
[b] Department of Building Materials and Engineering Geology, Budapesti University of Technology and Economics, Hungary
[c] Center for Advanced Cement-Based Materials, Northwestern University, Evanston, IL, United States

ARTICLE INFO

Article history:
Received 25 March 2011
Received in revised form 23 February 2012
Accepted 24 February 2012
Available online 14 March 2012

Keywords:
SCC
Formwork pressure
Limestone filler
Fly ash

ABSTRACT

Self-consolidating concrete (SCC) is a recently developed, innovative construction material. With use of SCC no additional compacting is necessary due to its high filling ability; as a result, the labor cost of compacting is economical. However, SCC may require stronger formwork that can resist the higher lateral pressure induced as compared to that for ordinary concrete. This study shows the effects of limestone filler or fly ash replacement on the formwork pressure and workability retention of a SCC mixture. Portland cement has been replaced with each of the powders in order to enhance its flowability and stability. It is observed that the powder replacement also increases the formwork pressure and decreases the workability retention. The effect of powder replacement on the formwork pressure is evaluated with a proposed two-function model, and discussed in comparison with the rheology of paste.

1. Introduction

The inception of self-consolidating concrete (SCC) can be traced to Japan [1] in the late 1980s, but the use of SCC in the ready-mixed concrete industry is still in its infancy. Maintaining the self-consolidating ability of ready-mixed SCC is not easy under construction site conditions. In addition, highly flowable SCC poured at a high placement rate can exert higher lateral pressure on formwork than conventional concrete [2,3]. The challenge of ready-mixed SCC is to create a balance between sufficient flowability and adequate resistance to segregation during transportation and placing. In order to address these problems, designers have employed high powder content and have used chemical admixtures, such as high-range water reducing admixture (HRWRA) and viscosity modifying admixture (VMA). The powder type used includes fly ash or limestone filler as well as Portland cement.

The operating mechanism of the fines in SCC has been investigated by many researchers and is outlined in the ACI 237 Committee report [4]. An increase of the powder volume improves the segregation stability of SCC [5]. Proper selection of powdered materials additionally enhances the packing density of solid particles, which enables reduction of water or the HRWRA dosage required to achieve inter-particle sliding, which is related to flowability [6]. Better packing not only leads to enhanced flowability but also provides higher compressive strength and durability due to the denser paste matrix [7,8]. Furthermore, pulverized limestone provides nucleation sites for hydration, and hence lends higher early age compressive strength [9]. The foregoing merits encourage the use of powder materials, and the ACI 237 Committee suggests 20–40% as the optimum ratio of inert or pozzolanic fines replaced for Portland cement, by weight. The fly ash replacement is sometimes more than 50% in special cases, and hence this is referred to as high-volume fly ash concrete [10].

Designing SCC entails finding the optimum state between self-consolidating (passing and filling ability) and other factors that poses challenging issues, such as segregation resistance and formwork pressure. Segregation resistance is the first and most important requirement for an SCC mixture, and hence it is not necessary to consider mixtures that do not meet a given stability criterion. Given that a SCC mixture is not segregated, the use of powder materials can be a means of controlling the workability (or workability retention) and formwork pressure. This study found that high powder content enhances workability and its retention but has a negative effect on formwork pressure. The increase of the formwork lateral pressure results in safety and economical problems. In an effort to acquire knowledge that will facilitate control between workability retention and formwork pressure, two important tests, slump flow and pressure response of SCC, have been carried out as part of this study. Both tests were applied to SCC mixtures containing commonly used powder materials: limestone filler or fly ash.

* Corresponding author. Address: 50 UNIST-gil, Eonyang-eup, Ulju-gun, Ulsan, 689-798, Republic of Korea. Tel.: +82 52 217 2817.
E-mail address: jaekim@unist.ac.kr (J.H. Kim).

0958-9465/$ - see front matter
http://dx.doi.org/10.1016/j.cemconcomp.2012.02.016

2. Experiments

2.1. Sample preparation

A total of nine concrete mixtures were tested, each prepared with Type I Portland cement, finely ground limestone filler, and fly ash. Their oxide compositions are listed in Table 1. The micro-sieving results and the Blaine values reported in Table 2 indicate that cement, pulverized limestone, and fly ash are in a decreasing order of fineness. The results of a laser particle size analysis, presented in Fig. 1, also confirmed that cement is finer than the other powders and a significant portion of finer particles is present in pulverized limestone. The Faunhofer method, using isopropyl alcohol as a dispersing medium, was employed in the particle size calculation.

Polycarboxylate-based HRWRA with a specific gravity of 1.00–1.07 was used as a chemical admixture. Aggregates used for producing concrete were prepared by sieving. The fine aggregate ranged between 0.15 mm (No. 100 sieve) and 4.75 mm (No. 4 sieve). The coarse aggregate was above the fine aggregate size and smaller than 9.5 mm (3/8 in sieve).

The concrete samples for the test were prepared with the compositions listed in Table 3. The use of a high powder content, 546 kg/m^3, provided sufficient resistance to segregation. The water-to-powder ratio was 37% by weight, and the paste volume calculated with the specific gravities of raw materials was approximately 39%. The control mixes, Group C, used cement only as powder. Three control mixes incorporating different HRWRA dosages were prepared for comparison. From the results, only Mix C8 incorporating 0.8% HRWRA could be considered as SCC showing adequate flowability.

Groups G and H are the samples in which cement was partially replaced with pulverized limestone and fly ash, respectively, maintaining the same water-to-powder ratio. The replacement ratios by weight were 30%, 40%, and 60%, in sequence. Replacing cement with fly ash or limestone filler further increases the paste volume of concrete, because the specific gravity of the replacements are lower than that of cement. The aggregate content by weight was constant for all samples, and was composed of 40% sand and 60% gravel. The main requirements when fabricating the samples were to attain a slump flow (d_f) of 72 ± 2 cm and no visual segregation, as defined by ASTM 1611-05 [11]. To fulfill these requirements, the dosage of HRWRA was adjusted for each mixture. A planetary mixer with a total mixing time of 10 min was used to produce about 15 L of SCC mixture.

Table 1
Oxide composition of the powders.

Oxide	Cement	Limestone filler	Fly ash
SiO_2	19.7	1.37	42.47
Al_2O_3	4.8	0.32	26.01
Fe_2O_3	2.8	0.119	8.44
CaO	63.9	54.38	14.01
MgO	2.5	0.67	3.15
SO_3	2.6	0.086	1.57
Equivalent alkalis	0.52	–	0.56
Free lime	1.57	Not available	Not available
Loss on ignition	2.4	Not available	1.05

Table 2
Physical characteristics of the powders.

Property	Cement	Limestone filler	Fly ash
Percent passing by No. 325 sieve (45 μm)	96.4	60.0	51.7
Blaine value (m^2/kg)	380	367	287
Specific gravity	3.15	2.72	2.44

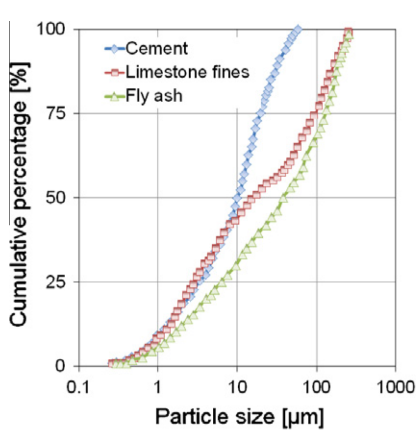

Fig. 1. Particle size distribution of the dry powders.

2.2. Formwork pressure test

The form pressure was measured by a laboratory device developed in a previous study [12]. The device is capable of simulating various casting situations, such as the change of concrete head heights and placement rates. The pressure vessel is a 1 cm thick, 15 cm inner diameter, 30 cm tall rigid metal cylinder that can be divided into two halves. The apparatus is capable of holding about 8 L of concrete and is thoroughly sealed when used. The vertical load was applied mechanically to the concrete sample surface, using a steel piston loaded by a closed-loop hydraulic testing machine, and a 22 kN load cell was fitted to measure the applied load. While vertical pressure was applied, the horizontal pressure was considered as the formwork pressure of the SCC sample. The horizontal pressure was gauged by a pressure cell of 350 kPa capacity positioned at the mid-height of the cylinder. While the vertical pressure was applied to a concrete sample, the change of horizontal pressure over time was recorded. The fresh concrete sample was subjected to a stepwise loading protocol for 2 h beginning at the age of 30 min; the vertical load was increased in every 30 min with 60 kPa.

The formwork pressure measurement was quantified using a two-function model previously developed by the authors [13–15]. The model analyzed the lateral-to-vertical pressure ratio with instantaneous and delayed responses. The instantaneous function β is defined as the pressure ratio at the time when vertical pressure is applied: $\beta(t') = \Delta\sigma_L(t')/\Delta\sigma_V(t')$, where $\Delta\sigma_L(t')$ and $\Delta\sigma_V(t')$ are the increase of lateral and vertical pressure at time t', respectively. The delayed function α indicates the sustaining portion of the pressure ratio over time $t > t'$, where t' is the loading time of pressure: $\alpha(t, t') = \Delta\sigma_L(t, t')/(\beta(t')\cdot\Delta\sigma_V(t'))$, where $\Delta\sigma_L(t, t')$ is the lateral pressure change over $t > t'$ with respect to $\Delta\sigma_V(t')$. The following equation establishes the relationship to calculate the lateral pressure $\sigma_L(t, t')$ if an increment of vertical pressure $\Delta\sigma_V(t')$ is applied:

$$\Delta\sigma_L(t,t') = \alpha(t,t')\beta(t')\Delta\sigma_V(t'). \quad (1)$$

Both functions are the material properties representing the formwork pressure behavior of an SCC mixture, and various experimental measurements showed that they could be simplified in the form of a linear function [14]. The instantaneous function linearly decreases with respect to the loading time $\beta(t') = 1 - b\cdot t'$, where the instantaneous coefficient of b is introduced. The delayed function also linearly decreases for the duration of loading $(t - t')$, and

Table 3
Mix proportion and test results for SCC.

Mix	Composition in kg for 1 m^{3a}							Test result			
	W	C	LF	FA	S	G	HRWRA	d_f (mm)	r_w (h^{-1})	b (h^{-1})	a (h^{-1})
C6	191	546	–	–	665	997	3.28 (0.6%)	445	–	0.288	0.313
C7	191	546	–	–	665	997	3.82 (0.7%)	600	–	0.284	0.483
C8	191	546	–	–	665	997	4.37 (0.8%)	700	1.34	0.117	0.415
G1	191	382	164 (30%)	–	665	997	4.37 (0.8%)	725	1.01	0.052	0.404
G2	191	328	218 (40%)	–	665	997	4.37 (0.8%)	730	1.06	0.015	0.191
G3	191	218	328 (60%)	–	665	997	3.28 (0.6%)	720	1.55	0.197	0.336
H1	191	382	–	164 (30%)	665	997	3.82 (0.7%)	750	1.19	0.061	0.498
H2	191	328	–	218 (40%)	665	997	3.82 (0.7%)	730	0.986	0.006	0.179
H3	191	218	–	328 (60%)	665	997	3.82 (0.7%)	710	0.977	0.004	0.413

[a] W, C, LF, FA, S, G, and HRWRA denote water, cement, limestone filler, fly ash, sand, gravel, and high-range water-reducing admixture, respectively.

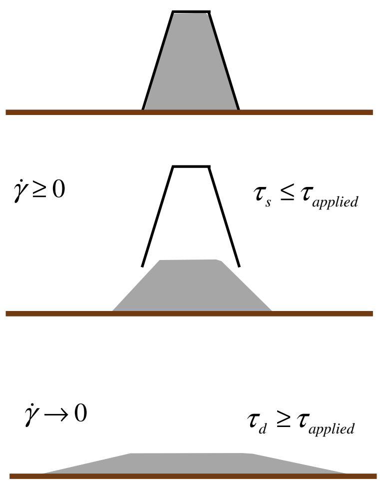

Fig. 2. Illustrative explanation of both yield stresses.

the rate of decrease is proportional to the loading time: $d\alpha/dt = -a^2 \cdot t'$. Consequently, the delayed function is simplified as $\alpha(t, t') = 1 - a^2 \cdot t' \cdot (t - t')$ with the delayed coefficient of a. The material properties for formwork pressure can be represented by the values of both coefficients, and the formwork pressure can be estimated by following the developed model presented in the Appendix.

Fig. 4 shows the applied and measured pressure in the vessel, where a stepwise vertical load was constructed with $\Delta\sigma_V(0) = \Delta\sigma_V(0.5) = \Delta\sigma_V(1.0) = \Delta\sigma_V(1.5) = 60$ kPa at time points of 0, 0.5, 1.0, and 1.5 h after casting, respectively. The values of $\beta(t')$ were evaluated with instantaneously measured horizontal pressure: $\beta(t') = \Delta\sigma_L(t', t')/\Delta\sigma_V(t')$. The evaluated data points are marked on Fig. 5a and c. The decreasing slope of the measured horizontal pressure determines the delayed function, and hence those values are calculated for each step: $d\alpha(t, t')/dt = \Delta\sigma_L(t, t')/(\beta(t') \cdot \Delta\sigma_V(t'))$ for $t' < t < t' + 0.5$. The data points for the delayed function are marked on Fig. 5b and d. Both functions are assumed to be a linear function of loading time and finally simplified by

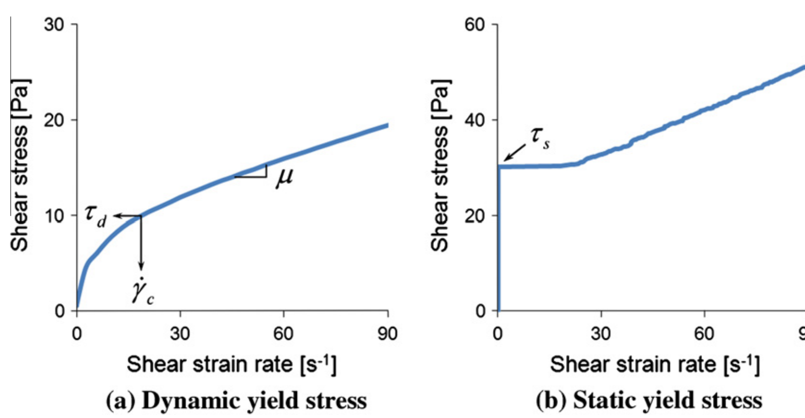

Fig. 3. Definition of both yield stresses.

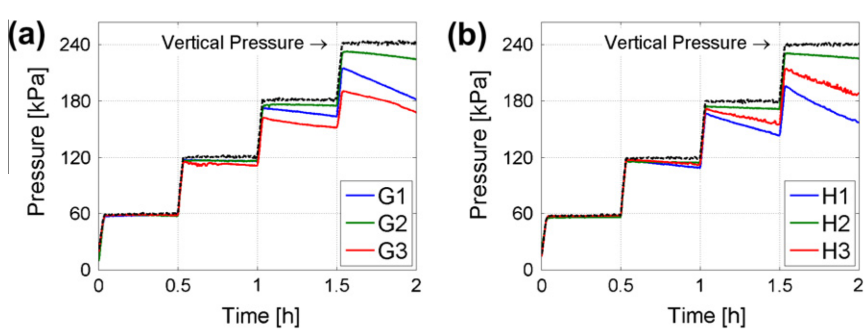

Fig. 4. Formwork pressure measurement of Groups G and H.

linear regression, as explained in the last paragraph. The linear coefficients (b and a) corresponding to β and α are reported in Table 3. The increase of each coefficient indicates a lower formwork pressure.

The formwork lateral pressure was obviously less than the hydrostatic pressure (equal to the applied vertical pressure), as shown in Fig. 4. The replacement generally increased the formwork pressure, which should be quantitatively evaluated based on the two-function model. It should be beforehand noticed that the HRWRA also affects the formwork pressure and that the instantaneous coefficient (b) is more important than the delayed coefficient (a) for determining the peak formwork pressure, as reported in a previous study [14]. Given that SCC mixtures have the same slump flow (the same level of flowability), a high HRWRA dosage decreases the instantaneous coefficient (b). A lower instantaneous coefficient by definition denotes higher formwork pressure.

The powder replacement effect was evaluated with control Mix C8, which displays sufficient slump flow (above 700 mm listed in Table 3) as an SCC mixture, as a reference. The limestone filler replacement increased the formwork pressure: Mixes G1 (30%) and G2 (40%) showed lower instantaneous coefficients, 0.052 and 0.015, respectively, than Mix C8 (b = 0.117). However, Mix G3 (60%, b = 0.197) provided a reduction of formwork pressure, which might be due to the use of lower HRWRA dosage [14]. The fly ash replacement also increased the formwork pressure, as seen from a comparison of Group H with control Mix C8. Each mix of Group H gave a lower instantaneous coefficient than that of Mix C8 even though a smaller dosage of HRWRA was needed to obtain enough slump flow over 700 mm. In other words, the HRWRA dosage for the SCC mix using fly ash is clearly reduced to obtain the target slump flow but the mix gives higher formwork pressure.

It should be noted that, in a previous study [12], when 30% of cement was replaced by Class F fly ash the formwork pressure was reduced and when Class C fly ash was used no difference was observed. In that study, the replacement ratio of fly ash was the volume ratio and the average sizes of the fly ash were finer than that of cement. Clearly the physical and chemical properties of fly ash influence the evolution of formwork pressure. Similarly, it should be noted that the limestone filler used in this study is coarser than that used in many prior studies.

2.3. Flowability retention

The SCC flowability was enhanced by powder replacement, as listed in Table 3. A small increase of the slump flow is found in Mixes G1 and G2, 725 mm and 730 mm, respectively, compared

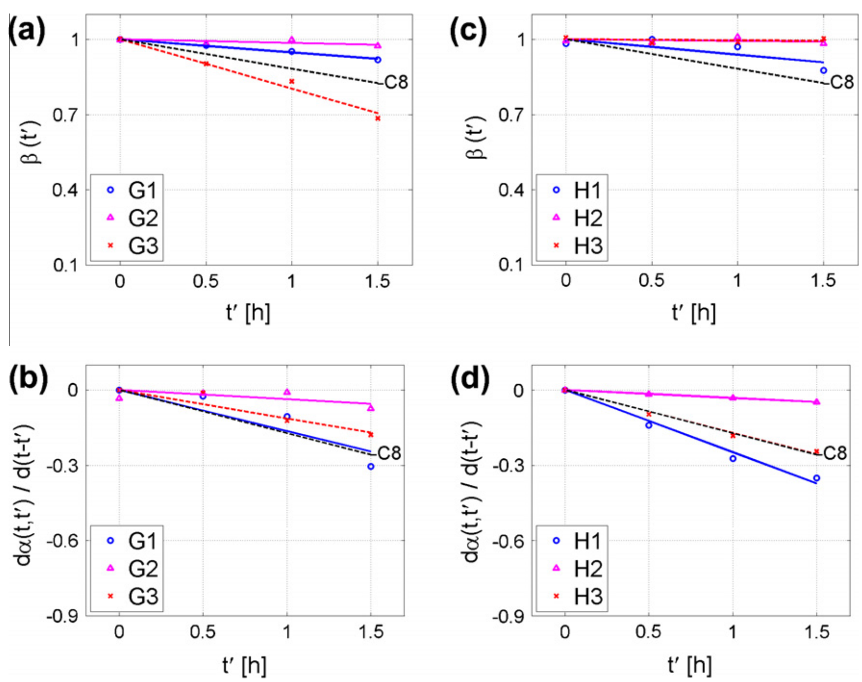

Fig. 5. Formwork pressure response of Groups G and H.

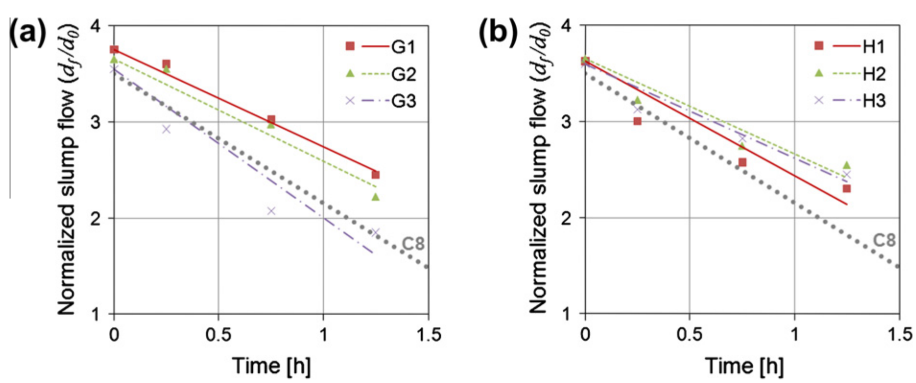

Fig. 6. Workability retention measurement of Group G and H.

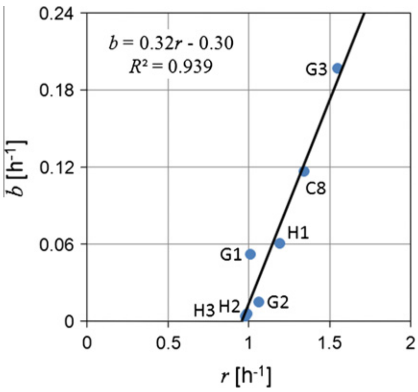

Fig. 7. Correlation between workability retention and formwork pressure.

to Mix C8 (700 mm) having the same dosage of HRWRA (0.8%). Mix G3, wherein cement was replaced with 60% limestone filler, exhibited 720 mm slump flow even with less HRWRA dosage (0.6%). All mixes in Group H also showed higher slump flow compared to Mix C7 having the same HRWRA dosage (0.7%, 600 mm).

The flowability retention was investigated by repeating the slump flow test at various intervals, up to 1.25 h after mixing. The mixes were kept in a covered container and then the slump flow test was performed again at 0.25 h, 0.75 h, and 1.25 h later. Each slump flow test was preceded by 2 min remixing. A quantitative flowability retention factor (r) was defined with the measured slump flow as follows: (1) the slump flow is first normalized with the diameter of the Abraham cone (d_0 = 200 mm); and (2) the data were then fitted into a linear function having a slope of $-r$. The regression used the following equation:

$$\frac{d_f(t)}{d_0} = \frac{d_f(0)}{d_0} - r \cdot t, \qquad (2)$$

where $d_f(t)$ is the slump flow measured at time t. An increase of r indicates poorer flowability retention.

The slump flow was repeatedly measured for 1.5 h after mixing, as shown in Fig. 6. The flowability retention factor (r), as reported in Table 3, was also influenced by the replacement ratio. Note that, in general, replacing cement with fly ash or limestone filler enhances the retention of slump flow. In Fig. 7, the retention factor (r) is compared with the instantaneous coefficient (b). A linear correlation exists between these two parameters; that is, with faster loss of slump flow (a higher retention factor), the amount of formwork pressure accordingly decreased (a higher value of instantaneous coefficient). In other words, the powder replacement has a negative effect on formwork pressure but helps to retain flowability for a longer time.

2.4. Rheological test for paste

The flowability of an SCC mixture is controlled by the rheological performance of the paste. The SCC mixes used the same amount of aggregates, and hence measuring the paste rheology does not deviate from the main focus of investigating the powder effect. For each mix the same water-to-powder ratio of 35% and 0.15% HRWRA dosage with respect to the powder weight were used. Table 4 shows the mix proportions of the paste samples. Paste Mixes LF30, LF40, and LF60 have the same limestone filler replacement ratio as SCC Mixes G1, G2, and G3, respectively. Group FA is also comparable to Group H. Approximately 1 L of paste was mixed using a small planetary mixer for about 10 min, following a similar mixing protocol to that described in a previous study [16].

Table 4
Mix proportion and test results of paste.

Mix	Composition in g for 1 L					Test result		
	W	C	LF	FA	HRWRA	d_f (mm)	τ_d (Pa)	τ_s (Pa)
CP	189	539	–	–	0.8 (0.15%)	186	32.1	2.41
LF10	189	485	54	–	0.8 (0.15%)	197	28.9	2.81
LF30	189	377	162	–	0.8 (0.15%)	235	17.1	2.71
LF40	189	323	216	–	0.8 (0.15%)	271	8.21	2.03
LF60	189	216	323	–	0.8 (0.15%)	227	15.0	1.28
FA10	189	485	–	54	0.8 (0.15%)	164	34.3	3.78
FA30	189	377	–	162	0.8 (0.15%)	213	20.7	2.51
FA40	189	323	–	216	0.8 (0.15%)	218	17.2	2.53
FA60	189	216	–	323	0.8 (0.15%)	307	3.88	8.03

We performed a mini-slump flow test on the paste samples using a Hägermann cone with dimensions of 100 mm-lower diameter, 70 mm-upper diameter, and 50 mm-height. The prepared sample showed high fluidity without any bleeding or water halo (good consistency). The test results obtained immediately after mixing are listed in Table 4.

The rheological properties, especially the yield stress, were measured with a rheometer (Haake RS 150, Thermo Fisher Scientific Inc.) with a concentric cylinder configuration having a gap size of 0.85 mm. The yield stress depends on the loading protocol applied to the sample. In this study, two states of yielding are defined: (1) static yield stress, τ_s, when a sample is in a stationary condition; and (2) dynamic yield stress, τ_d, measured when a sample is flowing.

The concepts of both yield stress definitions can be explained for the slump flow test, as illustrated in Fig. 2. The mixture used to fill the slump cone is placed at rest, and lifting the cone triggers the application of shear stress induced by its self-weight. Shear stress momentarily develops and the mixture yields to flow. The first yielding experienced by the mixture is due to the increased shear stress on the stationary mixture; hence it is referred to as 'static' yield stress. The shear stress-control protocol to measure the static yield stress reproduces the initial disturbance on the stationary mixture. Afterward, the mixture released from the cone spreads until its yield stress equilibrates with the applied shear stress, determined by its outward-sliding slope. The mixture experiences a second yielding, related to the final diameter of slump flow, while it is flowing (non-zero shear strain rate); this is known as 'dynamic' yield stress.

The dynamic yield stress is often used to characterize mixture rheology. The flow curve of a sample is obtained while the shear strain rate is increasing, and the yield stress is then determined from the measured flow curve. The shear rate-control protocol subjects a sample to flow even under the yield stress (see Fig. 3a). The concept of the dynamic yield stress has been widely adopted, for example, in the studies by Tattersall and Banfill [17] and De Larrard et al. [18]. One of the analysis methods was selected from a previous study [16]. The protocol starts with pre-shearing at a 600 s^{-1} shear rate and a 60 s rest period. The flow curve is then recorded while the shear strain rate is ramped up to 300 s^{-1} for 4 min. Fitting the measured flow curve into a modified Bingham model:

$$\tau = \tau_d \left(1 - \exp\left(\frac{3\dot{\gamma}}{\dot{\gamma}_c}\right)\right) + \mu\dot{\gamma}, \qquad (3)$$

determines the dynamic yield stress (τ_d), where $\dot{\gamma}_c$ and μ are the critical strain rates corresponding to the dynamic yield stress and the plastic viscosity, respectively. The dynamic yield stress refers to the front end of linear flow curve, and hence the cement paste shows Bingham fluid behavior (a constant plastic viscosity) only when $\tau > \tau_d$.

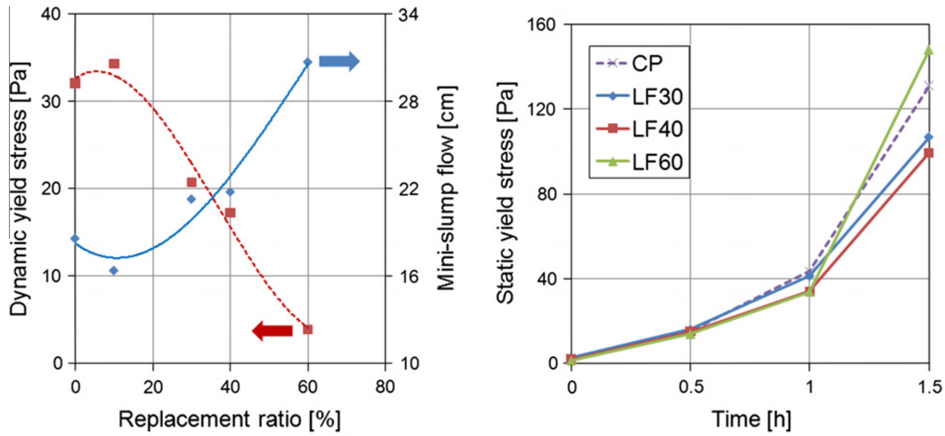

(a) Dynamic yield stress

(b) Static yield stress evolution

Fig. 8. Limestone filler replacement in the paste samples.

The static yield stress was measured by controlling the rate of shear stress, rather than the rate of shear strain. If the shear stress applied to samples is gradually increased, the angular velocity of the sensor is always zero until the applied shear stress exceeds the yielding of the sample at rest. The static yield stress was measured by ramping up the applied shear stress by 1 Pa/s. The shear stress increases continuously after yielding, and the time to approach the shear strain rate of 100 s^{-1}, varying according to the mix proportion, is in a range of 1–2 min. Fig. 3b shows the flow curve measured by the shear stress-control protocol. Both protocols were applied to all paste mixes, and the measurement results immediately after mixing are reported in Table 4.

In addition, the change of static yield stress with a rest period was also measured up to 2 h after mixing. A total of four replicated specimens from individual batches with the same mix proportion were used for measurements at 0 h, 0.5 h, 1.0 h, and 1.5 h. The replicated specimens were placed in the rheometer until each measurement time. The authors believe that the evolution of the static yield stress was related to the formwork pressure response, because a mixture placed in a formwork does not flow but instead stiffens in a stationary condition.

3. Discussion based on rheological measurement

3.1. Limestone filler

The hydrodynamic interaction of SCC constituents reportedly addresses the flowability of the mixture, because the granular skeleton volume fractions of SCC mixtures are generally smaller than the transition point from frictional interaction-dominant rheology [19]. The aggregate volume fraction of the Group C mixes was 61%, and the others mixes had lower values. It is again important to note that the powder replacement increased the volume of the paste. The increase of paste volume (a decrease of the aggregate volume fraction) is one of the possible explanations for the increased flowability.

In addition, the powder replacement is thought to change the paste itself. The hydrodynamic interaction is also governed by the properties of the suspension medium, the paste in this case. The powder replacement enhanced the consistency of the paste samples, as seen by the values of the mini-slump flow in Table 4. Even though the number of data is not sufficient to develop a regression model, the increase of mini-slump flow is clearly related to the decrease of the dynamic yield stress, as shown in Fig. 8a. The dynamic yield stress is inversely correlated with the mini-slump flow, as also reported in the literature [16,20]. The yield stress governing the flowability can be formulated as a function of φ/φ_m, similar to the Krieger–Dougherty equation for plastic viscosity, where φ and φ_m are the solid volume fraction and the packing density of a concentrated suspension, respectively [21–23]. The packing structure of the blend powder suspension is attributed to the particle size distribution, shape, water retention, and flocculating and agglomerating intensity [24,25]. Even though several techniques can be used to determine the packing density, including laser scanning microscopy [26], void fraction measurement [27], and viscosity-measured inverse estimation [28], it is still not easy to obtain consistent measurements. This is due to the inherent characteristics of cement-based materials, such as a shear-dependent flocculating microstructure. Despite the lack of packing information, it is likely that heterogeneous systems incorporating replacement powder provide a higher packing density than that of each constituent, as theoretically verified by Stovall et al. [29]. Widening the particle size distribution by blending two particles increases the packing density of pastes.

The pressure response is related to another measurement of rheology. The static yield stress follows the microstructure evolution of the paste samples. Interfacial forces due to physical and/or chemical reaction between particles, such as particle interlocking, provide a source of resistance against shear stress applied to the pastes at rest. The evolution of static yield stress is plotted in Fig. 8b. It can be seen that, compared to cement paste, 30% and 40% replacement of limestone filler gave a lower value of static yield stress while 60% replacement gave a higher value. The values

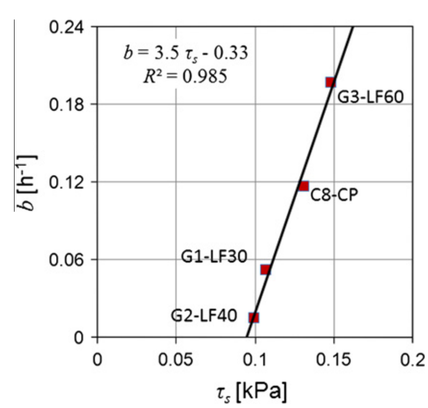

Fig. 9. Correlation between static yield stress and formwork pressure.

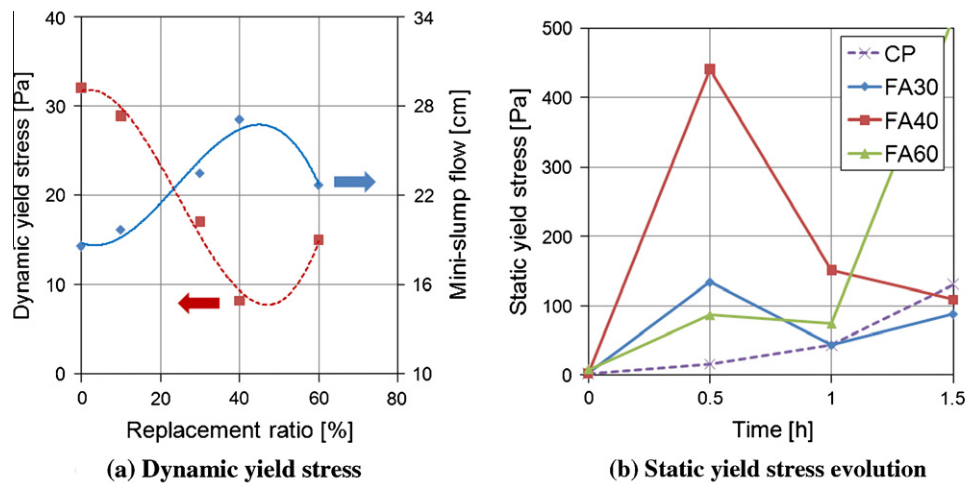

Fig. 10. Fly ash replacement in the paste samples.

of static yield stress at 1.5 h are correlated to the value of formwork pressure, as shown in Fig. 9. Slower stiffening of paste measured by the static yield stress leads to higher formwork pressure.

3.2. Fly ash

In the same manner as limestone filler, the fly ash replacement generally enhanced the flowability of cement paste as well as that of SCC. Fig. 10a shows an increase of mini-slump flow and a decrease of dynamic yield stress. However, the cement paste samples having fly ash did not show a clear trend in the evolution of static yield stress. The static yield stress quickly increased at 30 min and decreased afterward, as shown in Fig. 10b. Considering the very early age, the observed change leads us to infer that ettringite formation contributed to this phenomenon. The high lime (14%) and alumina (26%) content of the fly ash used also supports the argument of ettringite contribution. A considerable amount of aluminate would react with water and develop ettringite [30,31]. The needle-shape crystalline of ettringite anchors and locks the solid particles in a concentrated solution, resulting in thickening of the fresh mixture. Extremely high static yield stress was measured in some cases, including a value higher than 400 Pa for Mix FA40. The conversion of ettringite to monosulfate might account for the subsequent decrease of static yield stress. The lack of a sulfate phase causes ettringite to transform into monosulfate, which requires less sulfate phase for its stabilization [30,31]. Monosulfate crystallizes as thin hexagonal plates while the ettringite needles disappear, which weakens solid particle interlocking.

4. Conclusions

The use of powder materials is beneficial to produce inexpensive and environmentally-friendly SCC. Replacing Portland cement by limestone filler or fly ash increases the flowability and its retention of SCC. The enhanced flowability was investigated with the measured rheology of paste in this study. Replacing Portland cement with limestone filler increases the slump flow and decreases the dynamic yield stress as the replacement ratio increases. Using fly ash provides the optimum value of 40% replacement in terms of flowability. However, both powders produced an increase of formwork pressure over the control mix. The effect of powder replacement may vary according to the physical and chemical properties of the powder, but the overall trend is thought to be consistent. The flowability retention is improved at the expense of formwork pressure, which means an SCC mix showing good flowability retention gives high formwork pressure.

Acknowledgements

This work was supported by the year of 2011 Research Fund of the Ulsan National Institute of Science and Technology (UNIST), Hungarian American Enterprise Scholarship Fund, and Tennessee Valley Authority – Oak Ridge Associated Universities (TVA-ORAU, Coal Ash Research Grant 105866).

Appendix A

The Center for ACBM has conducted a series of studies in order to accurately evaluate and estimate formwork pressure exerted by SCC [32]. As a result of these investigations, an intrinsic model using two functions was proposed and verified for the purpose of the studies. A simplified model can provide a peak pressure if the instantaneous and delayed coefficients (b and a, respectively) are obtained for a given SCC mixture. The peak pressure would be 3.6wR when the casting time is longer than 7 h, but otherwise is given as a function of casting time (t):

$$p(t) = wR\left(t - \frac{b}{2}t^2 - \frac{a^2}{6}t^3 + \frac{ba^2}{12}t^4\right),$$

where w and R are the unit weight of concrete and the placement rate, respectively. If a column or wall having a height of h is cast, the total casting time would be $t = h/R$. For example, if SCC Mix G3 having $w = 25$ kN/m^3, $b = 0.197$ h^{-1}, and $a = 0.336$ h^{-1}, as seen in Table 3, is used, the calculation results of the peak formwork pressure will be as presented in the following table.

Placement rate	2 m/h	6 m/h
3 m tall member	61 kPa for 1.5 h casting	71 kPa for 0.5 h casting
5 m tall member	83 kPa for 2.5 h casting	113 kPa for 0.8 h casting
7 m tall member	88 kPa for 3.5 h casting	151 kPa for 1.2 h casting

References

[1] Okamura H, Ouchi M. Self-compacting concrete. J Adv Concr Technol 2003;1(1):5–15.
[2] Vanhove Y, Djelal C, Magnin A. Prediction of the lateral pressure exerted by self-compacting concrete on formwork. Mag Concr Res 2004;56(1):55–62.

[3] Billberg P, Silfwerbrand J, Österberg T. Form pressures generated by self-consolidating concrete. Concr Int 2005(October):35–42.
[4] ACI Committee 237. Self-consolidating concrete, ACI 237R-07. Farmington Hills: American Concrete Institute; 2007.
[5] Kwan KH, Ng YT. Improving the robustness of SCC by adding supplementary cementitious materials. Constr Build Mater 2010;24:2260–6.
[6] Ferraris CF, Obla KH, Hill R. The influence of mineral admixtures on the rheology of cement paste and concrete. Cem Concr Res 2001;31:245–55.
[7] Nehdi M, Pardhan M, Koshowski S. Durability of self-consolidating concrete incorporating high-volume replacement composite cements. Cem Concr Res 2004;34:2103–12.
[8] Sahmaran M, Yaman ÖI, Tokyay M. Transport and mechanical properties of self-consolidating concrete with high-volume fly ash. Cem Concr Compos 2009;31:99–106.
[9] Ye G, Liu X, de Schutter G, Poppe AM, Taerwe L. Influence of limestone powder used as filler in SCC on hydration and microstructure of cement pastes. Cem Concr Compos 2007;29:94–102.
[10] Malhotra VM, Mehta PK. High-performance, high-volume fly ash concrete for building sustainable and durable structures. Ottawa, Canada: Supplementary Cementing Materials for Sustainable Development, Inc.; 2008.
[11] ASTM C 1611-05. Standard test method for slump flow of self-consolidating concrete. American Society for Testing and Materials; 2005.
[12] Gregori A, Ferron R, Sun Z, Shah SP. Experimental simulation of self-consolidating concrete formwork pressure. ACI Mater J 2008;105(1):97–104.
[13] Kwon SH, Shah SP, Phung QT, Kim JH, Lee Y. Intrinsic model to predict formwork pressure. ACI Mater J 2010;107(1):20–6.
[14] Kim JH, Beacraft M, Kwon SH, Shah SP. Simple analytical model for formwork design of self-consolidating concrete. ACI Mater J 2011;108(1):38–45.
[15] Kim JH, Beacraft M, Shah SP. Effect of mineral admixtures on formwork pressure of self-consolidating concrete. Cem Concr Compos 2010;32:665–71.
[16] Tregger N, Ferrara L, Shah SP. Identifying viscosity of cement paste from mini-slump-flow test. ACI Mater J 2008;105(6):558–66.
[17] Tattersall GH, Banfill PFG. Rheology of fresh concrete. Pitman; 1983.
[18] De Larrard F, Ferraris CF, Sedran T. Fresh concrete: a Herschel–Bulkley material. Mater Struct 1998;31:494–8.
[19] Yammine J, Chaouche M, Guerinet M, Moranville M, Roussel N. From ordinary rheology concrete to self compacting concrete: a transition between frictional and hydrodynamic interactions. Cem Concr Res 2008;38:890–6.
[20] Roussel N, Coussot P. "Fifty-cent rheometer" for yield stress measurements: from slump to spreading flow. J Rheol 2005;49(3):705–18.
[21] Zhou JZQ, Fang T, Luo G, Uhlherr PHT. Yield stress and maximum packing fraction of concentrated suspensions. Rheol Acta 1995;34:544–61.
[22] Krieger IM, Dougherty TJ. A mechanism for non-Newtonian flow in suspensions of rigid spheres. J Rheol 1959;3(1):137–52.
[23] Struble LJ, Sun GK. Viscosity of Portland cement paste as a function of concentration. Adv Cem – Based Mater 1995;2:62–9.
[24] Hunger M, Bouwers HJH. Flow analysis of water–powder mixtures: application to specific surface area and shape factor. Cem Concr Compos 2009;31:39–59.
[25] Sakai E, Masuda K, Kakinuma Y, Aikawa Y. Effects of shape and packing density of powder particles on the fluidity of cement pastes with limestone powder. J Adv Concr Technol 2009;7(3):347–54.
[26] Ferron RD, Shah SP. The fresh state: from macroscale to microscale to nanoscale. Transp Res Rec 2010;2141:89–91.
[27] Wong HHC, Kwan AKH. Packing density of cementitious materials: Part 1 – measurement using a wet packing method. Mater Struct 2008;41:689–701.
[28] Tregger NA, Pakula ME, Shah SP. Influence of clays on the rheology of cement pastes. Cem Concr Res 2010;40(3):384–91.
[29] Stovall T, de Larrard F, Buil M. Linear packing density model of grain mixtures. Powder Technol 1986;48:1–12.
[30] Taylor HFW. Cement chemistry. London: Academic Press; 1990.
[31] Lea FM. Chemistry of cement and concrete. London: Edward Arnold Ltd.; 1956.
[32] Kwon SH, Kim JH, Shah SP. Development and applications of the intrinsic model for formwork pressure of self-consolidating concrete. Int J Concr Struct Mater 2012;6(1):31–40.